DALTON
FULL PAPER

Synthesis and characterization of a series of sterically-hindered amidines and their lithium and magnesium complexes

Joseph A. R. Schmidt [a,b] **and John Arnold** *[a,b]

[a] *Department of Chemistry, University of California at Berkeley, California, USA*
[b] *Chemical Sciences Division, Lawrence Berkeley National Laboratory, Berkeley, California 94720-1460, USA. E-mail: arnold@socs.berkeley.edu*

Received 22nd February 2002, Accepted 15th May 2002
First published as an Advance Article on the web 11th June 2002

A series of sterically hindered amidinate ligands containing terphenyl substituents at the carbon atom of the amidinate backbone have been synthesized in high yields; their lithium derivatives were prepared, including the first two examples of monodentate lithium amidinates. Additionally, two independent routes to magnesium amidinates have been developed, yielding both mono- and bis-amidinate magnesium complexes. The presence of substituents at the 2′, 6′, 2″, and 6″ positions on the terphenyl moieties attached to the amidinate backbone induces a strong steric effect. In the free-base amidines, equilibria between *E-syn* and *Z-syn* isomers were dependent upon the size of these groups, while in the lithium amidinates, the steric bulk of these ligands led to the formation of the first monodentate lithium amidinates. Finally, in the magnesium amidinates, short C–N bond lengths and reduced N–C–N bond angles were observed within the amidinate backbone.

Introduction

One of the challenging problems in organometallic and inorganic chemistry is the search for new ancillary ligands capable of supporting a wide variety of catalytic processes. Over the past several years, metal complexes employing amidinate ligands have been actively studied. These complexes have displayed a wide array of chemistry, and their use in important applications such as olefin polymerization has been described.[1–7] A major goal of research in this area involves the design and preparation of ligands that can be easily tuned, sterically and electronically, in order to form complexes that exhibit unusual structures and reactivity.

Over the past decade, our group has contributed widely to the field of amidinate chemistry, including investigations of tantalum,[8–10] zirconium,[11,12] titanium,[2,13,14] and scandium[15] species. Additionally, we have designed various new amidinate ligands, including tethered bis(amidinates),[3] amidinates with pendant donor arms,[16] and ferrocene-containing amidinate ligands.[17] In this report, we provide full details on the synthesis and structural properties of a series of new sterically-bulky amidines and their lithium and magnesium complexes.

A systematic investigation on the effects of steric bulk in amidinate ligands has been reported by Jordan, who described a series of mono-amidinate aluminium complexes.[18] It was found that as the steric bulk of the three substituents attached to the amidinate backbone is increased, the NCN angle of these ligands is reduced, as a direct result of the steric interactions between the three substituents (Fig. 1). In a subsequent paper, the syntheses of some amidinate ligands having very bulky substituents (adamantyl or 2,6-$^{i}Pr_2C_6H_3$) attached to the nitrogen atoms of the amidinate backbone were described (Fig. 2),[19] and it was shown that these species continued the trend of reduced NCN bond angles with bulkier substituents. Additional contributions to this field were supplied by Boeré who studied the effects of varying the carbon substituents on the ligands with bulky aryl groups attached to the nitrogen atoms of the amidinate backbone (Fig. 2).[20] Solution studies of

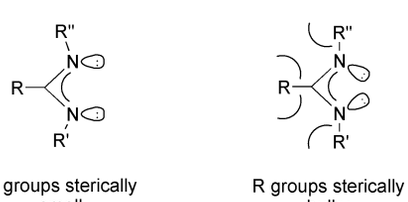

Fig. 1 Steric interaction between bulky substituents on the amidinate backbone results in smaller amidinate NCN bond angles.

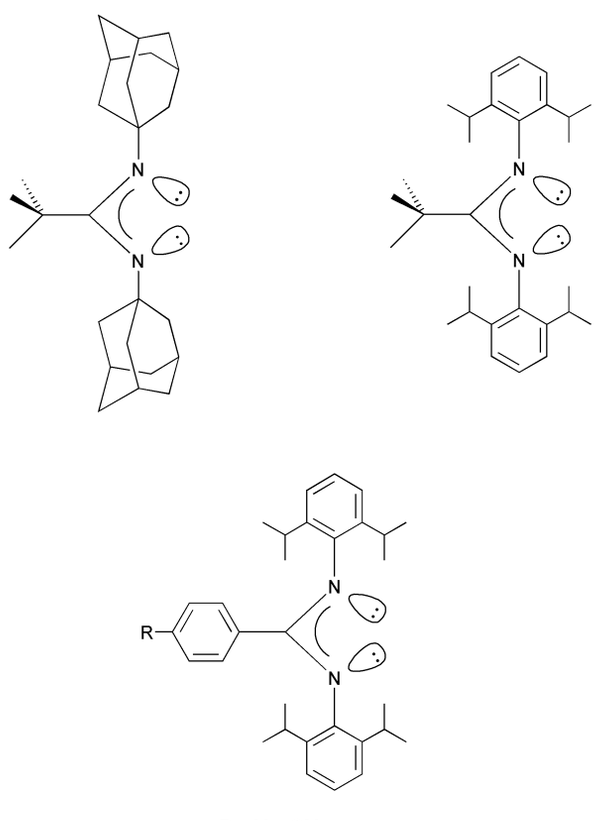

Fig. 2 Previous reports have detailed a number of sterically-bulky amidinates with large groups attached to the nitrogen atoms of the amidinate backbone.

 DOI: 10.1039/b202235b

these amidines showed slow isomerization about the backbone imine double bond, a phenomenon not observed in less sterically-hindered amidines.

Our initial contribution to the field of sterically-hindered amidinate ligands described the synthesis of amidinates having a bulky terphenyl substituent attached to the carbon atom of the amidinate backbone.[21] In this communication, we reported the free-base amidine and the lithium salt of the *N*,*N*′-diisopropyl[2,6-bis(mesityl)]benzamidine (**L_{Me}H**) ligand. This bowl-shaped amidine shows similar *cis-trans* isomerization in solution to that observed by Boeré, and its lithium salt features unprecedented monodentate coordination to lithium. Additionally, it proved possible to synthesize monoamidinate yttrium complexes using this very bulky amidinate ligand.[21]

Herein, we describe the synthesis of new sterically-bulky amidinate ligands, using alternate terphenyl groups as substituents at the carbon atom of the amidinate backbone.[22] The steric demands of these ligands are compared to those of the **L_{Me}H** ligand originally reported. The structural properties of the free-base and lithium salts of these ligands are presented, along with the crystal structures of each lithium amidinate. From this data, we show that the ortho-substituents on the external phenyl group of these terphenyl moieties (the 2′, 6′, 2″, and 6″ positions) play a strong role in the steric effect of these ligands. Additionally, two synthetic pathways for the formation of magnesium salts of these ligands are presented, one of which proves to be a novel route for the formation of mono-amidinate magnesium complexes.

Experimental

General considerations

Standard Schlenk-line and glove box techniques were used throughout. Pentane, hexanes, diethyl ether, and toluene were passed through a column of activated alumina and degassed with argon. THF was passed through a column of activated molecular sieves and degassed with argon. Tetramethylethylenediamine (TMEDA) was refluxed over molten sodium in a nitrogen atmosphere and distilled prior to use. Diisopropylcarbodiimide was dried over calcium hydride and distilled before use. Magnesium turnings were heated in an oven at 140 °C for one week prior to use. Dibutylmagnesium (1.0 M in heptane) and *n*-butyllithium (2.6 M in hexanes) were purchased as solutions and used as received. 2,6-bis(mesityl)iodobenzene, 2,6-bis(2,4,6-triisopropylphenyl)iodobenzene, 2,6-bis(2,4,6-triisopropylphenyl)phenyllithium etherate and 2,6-bis(4-*tert*-butylphenyl)iodobenzene were prepared as detailed previously.[23] C_6D_6 was vacuum transferred from sodium/benzophenone. Melting points were determined in sealed capillary tubes under nitrogen and are uncorrected. ^{1}H, ^{7}Li, and ^{13}C{^{1}H} NMR spectra were recorded in C_6D_6 at ambient temperature on a Bruker DRX-500 spectrometer, unless otherwise specified. ^{1}H NMR chemical shifts are given relative to C_6D_5H (δ 7.16). ^{7}Li NMR spectra are relative to an external LiCl (3M in D_2O) standard (δ 0.00). ^{13}C NMR chemical shifts are relative to C_6D_6 (δ 128.39). IR samples were prepared as Nujol mulls and taken between KBr plates. Elemental analyses were determined by the Microanalytical Laboratory of the College of Chemistry, University of California, Berkeley. Mass spectra are from the Mass Spectrometry Laboratory of the College of Chemistry, University of California, Berkeley, and in all cases employed electron impact conditions. Single crystal X-ray structure determinations were performed at CHEXRAY, University of California, Berkeley.

Preparations

***N*,*N*′-Diisopropyl[2,6-bis(mesityl)]benzamidine [L_{Me}H] (1).** A solution of *n*-BuLi (2.6 M in hexanes, 11.5 ml, 29.9 mmol) was added to a flask containing 2,6-bis(mesityl)iodobenzene (11.5 g, 26.1 mmol) as a slurry in pentane (150 ml) and the mixture was stirred for 4 h at ambient temperature. After removal of solvent under vacuum, the cream-colored solid was redissolved in diethyl ether (150 ml) and diisopropylcarbodiimide (4.5 ml, 3.65 g, 28.9 mmol) was added *via* syringe. The mixture was stirred overnight and then quenched by addition of water (2 ml). This was stirred a further 3 h before removal of all volatiles *in vacuo*. Water (30 ml) and CH_2Cl_2 (75 ml) were added and the organic extract was collected. The aqueous phase was extracted a second time with CH_2Cl_2 (75 ml). After drying the combined organics over anhydrous $MgSO_4$, these were filtered to obtain a yellow solution, which gave an oily material upon removal of solvent. Pentane (200 ml) was added to dissolve the oil and volatiles were again removed under vacuum to yield a cream-colored solid; (10.78 g, 94%); mp 92–94 °C; ^{1}H NMR (300 MHz) δ (*Z-syn*) 7.180 (t, 1 H, 5 Hz, *p*-Ph*H*), 6.967 (d, 2 H, 5 Hz, *m*-Ph*H*), 6.864 (s, 4 H, mes-Ar*H*), 3.439 (s, 1 H, N*H*), 3.420 (sept, 1 H, 6 Hz, Me_2CH), 3.257 (sept, 1 H, 6 Hz, Me_2CH), 2.279 (s, 12 H, *m*-mes-Ar*Me*), 2.208 (s, 6 H, *p*-mes-Ar*Me*), 0.872 (d, 6 H, 6 Hz, Me_2CH), 0.483 (d, 6 H, 6 Hz, Me_2CH); (*E-syn*) 7.140 (t, 1 H, 5 Hz, *p*-Ph*H*), 6.943 (d, 2 H, 5 Hz, *m*-Ph*H*), 6.846 (s, 2 H, mes-Ar*H*), 6.816 (s, 2 H, mes-Ar*H*), 4.015 (sept, 1 H, 6 Hz, Me_2CH), 3.484 (sept, 1 H, 6 Hz, Me_2CH), 3.464 (s, 1 H, N*H*), 2.172 (s, 6 H, mes-Ar*Me*), 2.162 (s, 6 H, mes-Ar*Me*), 2.143 (s, 6 H, mes-Ar*Me*), 0.962 (d, 6 H, 6 Hz, Me_2CH), 0.845 (d, 6 H, 6 Hz, Me_2CH); ^{13}C NMR δ 149.8 (C), 147.4 (C), 140.9 (C), 139.9 (C), 138.8 (C), 138.3 (C), 137.8 (C), 136.7 (C), 136.6 (C), 136.4 (C), 136.0 (C), 135.5 (C), 130.1 (CH), 128.7 (CH), 128.2 (CH), 128.0 (CH), 127.9 (CH), 127.5 (CH), 49.1 (CH), 46.2 (CH), 44.6 (CH), 44.5 (CH), 41.5 (CH), 41.4 (CH), 25.8 (CH_3), 23.6 (CH_3), 23.5 (CH_3), 23.3 (CH_3), 21.5 (CH_3), 21.3 (CH_3), 21.3 (CH_3), 21.2 (CH_3), 21.2 (CH_3), 21.1 (CH_3), 21.1 (CH_3), 21.0 (CH_3); MS: *m*/*z* 440.5 (M^+); IR: 3463 (w), 3427 (w), 2729 (w), 1942 (w), 1878 (w), 1814 (w), 1725 (w), 1667 (s), 1647 (s), 1625 (m), 1612 (m), 1573 (w), 1489 (s), 1331 (w), 1312 (m), 1263 (s), 1182 (m), 1169 (w), 1115 (m), 1069 (w), 1034 (m), 850 (s), 809 (w), 789 (w), 763 (m), 742 (w) cm^{-1}. Anal. Calc. for $C_{31}H_{40}N_2$: C, 84.49; H, 9.15; N, 6.36. Found: C, 84.26; H, 9.45; N, 6.56%.

***N*,*N*′-Diisopropyl[2,6-bis(2,4,6-triisopropylphenyl)]benzamidine [L_{Pr}H] (2).** A small flask was charged with 2,6-bis-(2,4,6-triisopropylphenyl)phenyllithium etherate (2.48 g, 4.41 mmol) and diethyl ether (30 ml). This was cooled to −78 °C and a solution of diisopropylcarbodiimide (0.6 g, 4.8 mmol) in diethyl ether (30 ml) was added *via* cannula. This was stirred and slowly warmed to room temperature overnight. An excess of water was added and the mixture was stirred for 1 h further. After removal of volatiles under vacuum, water and hexanes were added (50 ml each) and the organic layer that separated was collected. The aqueous phase was extracted with additional portions of hexanes (3 × 50 ml), and the combined organic extracts were dried over anhydrous $MgSO_4$. After filtration, the solution was concentrated to saturation and cooled to −30 °C, resulting in formation of colorless crystals. The crystals were filtered and dried *in vacuo*. A second crop was obtained similarly; (2.14 g combined, 80%); mp 159–160 °C; ^{1}H NMR δ 7.216 (d, 2H, 7.5 Hz, *m*-Ph*H*), 7.158 (s, 4H, ^{i}Pr$_3$-Ar*H*), 7.156 (t, 1H, 7.5 Hz, *p*-Ph*H*), 3.608 (d, 1H, 10 Hz, N*H*), 3.577 (sept, 1H, 6.5 Hz, C=NC*H*Me_2), 3.409 (doublet of septets, 1H, $^3J_{HCCH}$ = 6.5 Hz, $^3J_{HNCH}$ = 10 Hz, C-NHC*H*Me_2), 3.061 (sept, 4H, 7 Hz, *o*-Me_2CH), 2.871 (sept, 2H, 7 Hz, *p*-Me_2CH), 1.419 (d, 12H, 7 Hz, Ar-*Me*$_2$CH), 1.291 (d, 12H, 7 Hz, Ar-*Me*$_2$CH), 1.130 (d, 12H, 7 Hz, Ar-*Me*$_2$CH), 0.803 (d, 6H, 6.5 Hz, NCH*Me*$_2$), 0.492 (d, 6H, 6.5 Hz, NCH*Me*$_2$); ^{13}C NMR δ 148.3 (C), 147.4 (C), 147.2 (C), 140.5 (C), 139.7 (C), 137.0 (C), 130.8 (CH), 126.3 (CH), 120.7 (CH), 46.7 (CH), 45.1 (CH), 34.9 (CH), 31.0 (CH), 26.4 (CH_3), 24.5 (CH_3), 23.8 (CH_3), 23.5 (CH_3), 22.9 (CH_3); MS: *m*/*z* 608 (M^+); IR: 3404 (m), 1764 (w), 1652 (s), 1606 (m),

1567 (w), 1488 (s), 1379 (s), 1317 (m), 1260 (m), 1183 (w), 1167 (m), 1118 (m), 1102 (m), 1069 (m), 1053 (m), 940 (w), 921 (w), 875 (m), 851 (w), 805 (m), 778 (w), 765 (m), 719 (w), 706 (w), 650 (w), 582 (w), 533 (w), 521 (w), 481 (w), 440 (w) cm^{-1}. Anal. Calc. for $C_{43}H_{64}N_2$: C, 84.81; H, 10.59; N, 4.60. Found: C, 84.63; H, 10.64; N, 4.39%.

***N*,*N*′-Diisopropyl[2,6-bis(4-*tert*-butylphenyl)]benzamidine [$L_{Bu}H$] (3).** A 500 ml flask was charged with 2,6-bis(4-*tert*-butylphenyl)iodobenzene (6.73 g, 14.4 mmol) and pentane (400 ml). A solution of *n*-BuLi (2.6 M in hexanes, 5.6 ml, 14.6 mmol) was added *via* syringe and the suspension was stirred for 4 h at room temperature. The solvent was removed under vacuum and the solid was dissolved in diethyl ether (350 ml). Diisopropylcarbodiimide (4 ml, 3.2 g, 26 mmol, 1.8 eq) was added *via* syringe and the reaction was stirred overnight. After quenching with excess water, the reaction was pumped down to a white solid. Water (100 ml) was added, the mixture was extracted with CH_2Cl_2 (3 × 100 ml), and the combined organic fractions were dried over anhydrous $MgSO_4$. The solution was filtered and the solvent was removed under vacuum to yield a colorless product; (5.86 g, 87%); mp 129–130 °C; ^{1}H NMR δ 7.591 (d, 4H, 8 Hz, tol-Ar*H*), 7.381 (d, 4H, 8 Hz, tol-Ar*H*), 7.375 (d, 2H, 8 Hz, *m*-Ph*H*), 7.240 (t, 1H, 8 Hz, *p*-Ph*H*), 4.092 (sept, 1H, 6 Hz, Me_2CH), 3.385 (sept, 1H, 6 Hz, Me_2CH), 3.138 (br, 1H, N*H*), 1.255 (s, 18H, Me_3C), 0.807 (d, 6H, 6 Hz, Me_2CH), 0.791 (d, 6H, 6 Hz, Me_2CH); ^{13}C NMR δ 152.2 (C), 150.9 (C), 141.9 (C), 139.2 (C), 134.7 (C), 129.7 (CH), 129.6 (CH), 129.2 (CH), 125.6 (CH), 50.4 (CH), 42.3 (CH), 34.9 (C), 31.8 (CH_3), 25.4 (CH_3), 22.8 (CH_3); MS: *m*/*z* 468 (M^+); IR: 3435 (m), 2360 (w), 2342 (w), 1636 (s), 1585 (w), 1513 (m), 1311 (w), 1261 (s), 1203 (w), 1179 (m), 1098 (m), 1019 (m), 838 (m), 801 (s), 765 (m), 686 (w), 614 (w), 600 (w), 577 (m) cm^{-1}. Anal. Calc. for $C_{33}H_{44}N_2$: C, 84.56; H, 9.46; N, 5.98. Found: C, 84.67; H, 9.32; N, 5.94%.

***N*,*N*′-Diisopropyl[2,6-bis(mesityl)benzamidinatolithium-(TMEDA) [L_{Me}Li(TMEDA)] (4).** A suspension of $L_{Me}H$ (15.2 g, 34.5 mmol) in diethyl ether (300 ml) was treated with *n*-BuLi (2.6 M in hexanes, 13.5 ml, 35.1 mmol) and allowed to stir for 14 h. To this was then added TMEDA (6 ml) *via* syringe. After stirring for 3 h, the solution was filtered and concentrated to 90 ml. Upon cooling to −40 °C overnight, colorless crystals formed. After filtration and drying under vacuum, the crystalline product was isolated; (14.6 g, 75%); mp 234–237 °C; ^{1}H NMR δ 7.244 (t, 1 H, 7.5 Hz, *p*-Ph*H*), 7.096 (d, 2 H, 7.5 Hz, *m*-Ph*H*), 6.929 (s, 2 H, mes-Ar*H*), 6.888 (s, 2 H, mes-Ar*H*), 3.635 (sept, 1 H, 6 Hz, Me_2CH), 2.978 (s, 6 H, mes-Ar*Me*), 2.798 (s, 6 H, mes-Ar*Me*), 2.377 (sept, 1 H, 6 Hz, Me_2CH), 2.237 (s, 6 H, mes-Ar*Me*), 1.533 (s, 12 H, NCH_3), 1.452 (s, 4 H, NCH_2), 1.193 (d, 6 H, 6 Hz, Me_2CH), 0.851 (d, 6 H, 6 Hz, Me_2CH); ^{7}Li NMR δ 1.213; ^{13}C NMR δ 163.8 (N*C*N), 144.7 (C), 142.0 (C), 141.3 (C), 140.8 (C), 136.7 (C), 135.3 (C), 129.8 (CH), 128.7 (CH), 127.6 (CH), 125.7 (CH), 56.7 (NCH_2), 48.9 (CH), 48.1 (CH), 45.7 (CH_3), 30.3 (CH_3), 24.7 (CH_3), 23.9 (CH_3), 22.7 (CH_3), 21.7 (CH_3); IR: 2799 (m), 2730 (w), 1526 (s), 1376 (s), 1367 (s), 1311 (w), 1289 (w), 1270 (w), 1148 (w), 1131 (w), 1102 (w), 1039 (m), 1019 (w), 976 (w), 946 (w), 855 (w), 793 (w), 758 (w), 503 (w) cm^{-1}. Anal. Calc. for $C_{37}H_{55}N_4Li$: C, 78.96; H, 9.85; N, 9.95. Found: C, 78.66; H, 10.01; N, 9.56%.

***N*,*N*′-Diisopropyl[2,6-bis(2,4,6-triisopropylphenyl)]benzamidinatolithium(TMEDA) [L_{Pr}Li(TMEDA)] (5).** A solution of *n*-BuLi (0.8 ml, 2.8 M in hexanes, 2.24 mmol) was added to a flask charged with **2** (0.58 g, 0.95 mmol) and diethyl ether (40 ml). TMEDA (0.4 ml, 308 mg, 2.65 mmol) was added *via* syringe. The resulting yellow solution was stirred for 90 min and then pumped down to a foamy solid under vacuum. The solid was extracted with pentane (15 ml) and filtered. The resulting clear yellow solution was concentrated *in vacuo* to a volume of 5 ml and slowly cooled to −40 °C, resulting in the formation of pale yellow crystals. The product was isolated by filtration and dried under vacuum; (216 mg, 31%); mp 202–205 °C; ^{1}H NMR δ 7.424 (d, 2H, 7.5 Hz), 7.277 (t, 1H, 7.5 Hz), 7.221 (br, 4H), 3.714 (sept, 2H, 6.5 Hz), 3.544 (sept, 2H, 6.5 Hz), 3.489 (sept, 1H, 6.5 Hz), 2.955 (sept, 2H, 7 Hz), 2.743 (br, 1H), 1.661 (s, 12H), 1.639 (d, 6H, 6.5 Hz), 1.454 (s, 4H), 1.446 (d, 6H, 6.5 Hz), 1.367 (d, 18H, 7 Hz), 1.200 (d, 6H, 6.5 Hz), 0.890 (d, 6H, 6.5 Hz), 0.621 (d, 6H, 6.5 Hz); ^{7}Li NMR δ 1.560 (br); ^{13}C NMR δ 162.3 (C), 150.0 (C), 146.3 (C), 145.0 (C), 141.3 (C), 140.6 (C), 139.7 (C), 131.7 (CH), 123.6 (CH), 120.1 (CH), 119.7 (CH), 56.7 (CH_2), 46.8 (CH), 46.4 (CH_3), 46.3 (CH_3), 34.9 (CH), 30.9 (CH), 30.6 (CH), 28.7 (CH_3), 27.6 (CH_3), 26.2 (CH_3), 24.7 (CH_3), 24.6 (CH_3), 24.0 (CH_3), 23.6 (CH_3); IR: 1649 (w), 1605 (w), 1565 (m), 1512 (s), 1408 (w), 1353 (s), 1344 (s), 1318 (s), 1289 (m), 1269 (w), 1248 (w), 1180 (w), 1158 (m), 1105 (m), 1068 (w), 1032 (w), 1018 (m), 972 (m), 948 (m), 870 (m), 804 (w), 792 (w), 772 (m), 714 (w), 650 (w), 616 (w) cm^{-1}. Anal. Calc. for $C_{49}H_{79}N_4Li$: C, 80.50; H, 10.89; N, 7.66. Found: C, 80.42; H, 10.53; N, 7.39%.

***N*,*N*′-Diisopropyl[2,6-bis(4-*tert*-butylphenyl)]benzamidinatolithium(TMEDA) [L_{Bu}Li(TMEDA)] (6).** A 1 L flask was charged with 2,6-bis(4-*tert*-butylphenyl)iodobenzene (20 g, 43 mmol) and pentane (800 ml). A solution of *n*-BuLi (2.6 M in hexanes, 17 ml, 44 mmol) was added *via* syringe and the suspension was stirred for 4 h at room temperature. The solvent was removed under vacuum and the solid was suspended in diethyl ether (500 ml). Diisopropylcarbodiimide (10 ml, 8.1 g, 64 mmol, 1.5 eq) was added *via* syringe and the reaction was stirred overnight. TMEDA (10 ml) was then added *via* syringe and the mixture was stirred for 15 min. The solution was filtered through Celite and concentrated under vacuum to 325 ml. Cooling to −30 °C produced a large amount of yellow crystalline solid which was isolated by filtration and dried *in vacuo*. Concentration and cooling of the supernatant yielded a second crop of product in similar fashion; (19.0 g combined, 75%); mp 182 °C (dec.); ^{1}H NMR δ 8.144 (d, 4H, 8.5 Hz, tol-Ar*H*), 7.585 (d, 2H, 7.5 Hz, *m*-Ph*H*), 7.405 (d, 4H, 8.5 Hz, tol-Ar*H*), 7.308 (t, 1H, 7.5 Hz, *p*-Ph*H*), 3.362 (sept, 2H, 6 Hz, Me_2CH), 2.115 (s, 12H, N*Me*), 1.842 (br, 4H, NCH_2), 1.347 (s, 18H, Me_3C), 0.772 (d, 12H, 6 Hz, Me_2CH); ^{7}Li NMR δ 2.417; ^{13}C NMR δ 169.6, 149.4, 140.8, 140.0, 136.9, 130.8, 129.3, 127.6, 124.8, 47.7, 46.2, 34.8, 32.0, 31.8, 28.2; IR: 3052 (m), 2791 (m), 1911 (w), 1866 (w), 1795 (w), 1672 (w), 1611 (w), 1574 (w), 1512 (m), 1407 (m), 1383 (m), 1333 (s), 1290 (w), 1268 (m), 1203 (m), 1179 (w), 1158 (m), 1130 (m), 1111 (w), 1098 (w), 1065 (w), 1039 (w), 1022 (m), 997 (m), 945 (m), 843 (m), 803 (m), 792 (w), 770 (s), 747 (w), 719 (w), 685 (w), 650 (w), 617 (w), 575 (m), 554 (m), 439 (w) cm^{-1}. Anal. Calc. for $C_{39}H_{59}N_4Li$: C, 79.28; H, 10.07; N, 9.48. Found: C, 78.89; H, 10.25; N, 9.12%.

Bis[*N*,*N*′-diisopropyl(2,6-bis-mesityl)benzamidinato]-magnesium(II) [$(L_{Me})_2$Mg] (7). A solution of $L_{Me}H$ (1.00 g, 2.27 mmol) in toluene (75 ml) was cooled to −78 °C and a solution of dibutylmagnesium was added (1.0 M in heptane, 1.1 ml, 1.1 mmol). The resulting mixture was stirred overnight, while slowly warming to room temperature. The solvent was removed under vacuum, the residue was treated with hexanes (70 ml), and solvent again removed *in vacuo*. The resulting solid was extracted with hexanes (100 ml), and after filtration, the solution was concentrated and slowly cooled to −30 °C overnight. The resulting colorless crystals were isolated by filtration and were dried under vacuum; (474 mg, 46%); mp 179–181 °C; ^{1}H NMR δ 7.08 (t, 2H, 7.5 Hz, *p*-Ph*H*), 7.00 (d, 4H, 7.5 Hz, *m*-Ph*H*), 6.83 (s, 8H, mes-Ar*H*), 3.26 (sept, 4H, 5.8 Hz, Me_2CH), 2.27 (s, 24H, *o*-mes-Ar*Me*), 2.14 (s, 12H, *p*-mes-Ar*Me*), 0.66 (d, 24H, 5.8 Hz, Me_2CH); ^{13}C NMR δ 170.1 (C), 141.0 (C), 139.4 (C), 136.6 (C), 136.2 (C), 131.9 (CH), 128.3 (CH), 127.2 (C), 126.9 (CH), 45.0 (CH), 27.3 (CH_3), 22.3 (CH_3),

Table 1 Crystal data and collection parameters

Compound	**1**	**5**·1/2C_5H_{12}	**6**	**7**	**8**
Formula	$C_{31}H_{40}N_2$	$C_{51.5}H_{85}N_4Li$	$C_{39}H_{59}N_4Li$	$C_{62}H_{78}N_4Mg$	$C_{41}H_{60.5}N_2O_2MgI$
Formula weight	440.67	767.21	590.86	903.63	764.65
Space group	$P2_1/c$ (no. 14)	$P2_1/n$ (no. 14)	$P2_1/n$ (no. 14)	$C2/c$ (no. 15)	P_1/n (no. 14)
Temperature/°C	−161	−142	−117	−120	−105
a/Å	18.458(2)	12.4691(4)	13.610(1)	16.048(2)	8.9748(2)
b/Å	8.976(1)	22.9058(7)	15.425(1)	15.578(2)	19.9016(5)
c/Å	16.529(2)	17.6839(4)	18.541(1)	25.560(3)	23.4606(5)
β/°	91.458(1)	100.968(1)	100.170(1)	98.319(2)	99.864(1)
V/Å^3	2737.7(4)	4958.5(2)	3831.1(3)	6323(1)	4128.4(1)
Z	4	4	4	4	4
Diffractometer	Siemens SMART	Siemens SMART	Siemens SMART	Siemens SMART	Siemens SMART
Radiation (λ = 0.71069 Å)	Mo-Kα	Mo-Kα	Mo-Kα	Mo-Kα	Mo-Kα
Monochromator	Graphite	Graphite	Graphite	Graphite	Graphite
Detector	CCD area detector	CCD area detector	CCD area detector	CCD area detector	CCD area detector
Scan type, width/°	ω, 0.3	ω, 0.3	ω, 0.3	ω, 0.3	ω, 0.3
Scan speed/s per frame	20.0	20.0	20.0	25.0	10.0
Reflections measured	Hemisphere	Hemisphere	Hemisphere	Hemisphere	Hemisphere
Crystal dimensions/mm	0.33 × 0.32 × 0.25	0.45 × 0.23 × 0.10	0.41 × 0.30 × 0.19	0.21 × 0.19 × 0.10	0.36 × 0.17 × 0.15
Reflections measured	15547	22196	17200	11483	18631
Unique reflections	5227	8343	6630	3473	7129
Observations	2056	3835	2410	1289	3017
Parameters	299	523	397	255	450
R, R_w, R_{all}	0.076; 0.082; 0.164	0.056; 0.060; 0.118	0.052; 0.058; 0.133	0.1333;0.162,0.175	0.033;0.044;0.088

20.5 (CH_3); MS: *m*/*z* 903 (M^+); IR: 1608 (w), 1428 (s), 1312 (s), 1261 (m), 1239 (w), 1140 (w), 1101 (w), 1029 (w), 1008 (w), 849 (m), 773 (m), 738 (w), 638 (w), 591 (w), 582 (w), 571 (w), 458 (w) cm^{-1}. Anal. Calc. for $C_{62}H_{78}N_4Mg$: C, 82.41; H, 8.70; N, 6.20. Found: C, 82.33; H, 9.42; N, 5.88%.

***N*,*N*′-Diisopropyl[2,6-bis(4-*tert*-butylphenyl)]benzamidinatomagnesium(II) iodide bis(tetrahydrofuranate) [L_{Bu}MgI(THF)$_2$] (8).** A 100 ml flask was charged with Mg turnings (0.090 g, 3.7 mmol) and 2,6-bis(4-*tert*-butylphenyl)iodobenzene (1.0 g, 2.1 mmol). To this, THF (40 ml) was added, in addition to a few crystals of I_2 (to initiate the Grignard reaction) and the reaction was heated to reflux for 3 h causing the solution to turn grey. After cooling to room temperature, diisopropylcarbodiimide (0.4 ml, 324 mg, 2.6 mmol) was added *via* syringe and the reaction mixture was stirred at ambient temperature for 14 h. After removal of solvent under vacuum, pentane (40 ml) was added and this too was removed *in vacuo*. The grey-white solid was washed with pentane (40 ml) and then extracted with diethyl ether (40 ml, 2 × 15 ml). The ether extracts were combined, and the solution was then concentrated and cooled to −30 °C, yielding colorless crystalline plates. These were isolated by filtration and dried under vacuum. A second crop of product was isolated in similar fashion by concentration of the supernatant solution; (853 mg combined, 53%); mp 302–304 °C; ^{1}H NMR δ 7.80 (d, 4H, 8 Hz, tol-Ar*H*), 7.47 (d, 4H, 8 Hz, tol-Ar*H*), 7.45 (d, 2H, 8 Hz, *m*-Ph*H*), 7.25 (t, 1H, 8 Hz, *p*-Ph*H*), 3.72 (br, 8H, OCH_2), 3.34 (sept, 2H, 6 Hz, Me_2CH), 1.31 (s, 18H, Me_3C), 1.30 (br, 8H, OCH_2CH_2), 0.774 (d, 12H, 6 Hz, Me_2CH); ^{13}C NMR δ 173.3 (C), 150.6 (C), 141.0 (C), 139.5 (C), 132.2 (C), 130.0 (CH), 129.9 (CH), 129.2 (CH), 126.0 (CH), 69.9 (CH_2), 46.8 (CH), 35.0 (C), 31.9 (CH_3), 26.8 (CH_3), 25.5 (CH_2); IR: 1630 (w), 1585 (w), 1514 (w), 1441 (s), 1342 (s), 1311 (w), 1271 (w), 1225 (w), 1203 (w), 1182 (w), 1165 (w), 1144 (w), 1117 (w), 1099 (w), 1032 (m), 877 (m), 854 (w), 843 (w), 806 (m), 777 (m), 687 (w), 619 (w), 579 (m) cm^{-1}. Anal. Calc. for $C_{41}H_{59}N_2O_2MgI$: C, 64.53; H, 7.79; N, 3.67. Found: C, 64.15; H, 7.89; N, 3.37.

X-Ray crystallography

A summary of crystal data and collection parameters for the crystal structures of **1**, **5**, **6**, **7** and **8** are given in Table 1. Details of individual data collection and solution are given below, while complete structural data has been submitted to CCDC. ORTEP diagrams were created using the ORTEP-3 software package.[24]

For each sample, a crystal was mounted on a glass capillary using Paratone-N hydrocarbon oil. The crystal was transferred to a Siemens SMART[25] diffractometer/CCD area detector, centered in the X-ray beam, and cooled using a nitrogen-flow low-temperature apparatus that had been previously calibrated by a thermocouple placed at the same position as the crystal. A least-squares refinement on data from 60 sample frames allowed determination of cell constants and the orientation matrix. An arbitrary hemisphere of data was collected using 0.3° ω-scans, and the data were integrated by the program SAINT.[26] The final unit cell parameters were determined by least-squares analysis of the reflections with $I > 10\sigma(I)$. Data analysis using Siemens XPREP[27] determined the space group. The data were corrected for Lorentz and polarization effects, but no correction for crystal decay was applied. Equivalent reflections were averaged, and the structure was solved by direct methods[28] and expanded using Fourier techniques,[29] all within the teXsan[30] software package. The non-hydrogen atoms were refined anisotropically. Hydrogen atoms were included as fixed atoms but not refined. The weighting schemes were based on counting statistics and included a factor (p = 0.030) to reduce the weight of intense reflections. The analytical forms of the scattering factor tables for the neutral atoms were used,[31] and all scattering factors were corrected for both the real and imaginary components of anomalous dispersion.[32]

Complex 1. X-Ray quality crystals were grown from a saturated pentane solution that was cooled to −30 °C. The final cycle of full-matrix least squares refinement [minimizing the quantity $\Sigma w(|F_o| - |F_c|)^2$, where w is the weight of a given observation] was based on 2056 observed reflections [$I > 3.00\ \sigma(I)$] and 299 variable parameters and converged yielding final residuals:[33] R = 0.076, R_w = 0.082, and GOF = 2.44.

Complex 5. X-Ray quality crystals were grown from a saturated pentane solution that was cooled to −40 °C. One molecule of pentane was incorporated in the crystal lattice, located on an inversion center and disordered over two positions. The final cycle of full-matrix least squares refinement [minimizing the quantity $\Sigma w(|F_o| - |F_c|)^2$, where w is the weight of a given observation] was based on 3835 observed reflections [$I > 3.00\ \sigma(I)$] and 523 variable parameters and converged yielding final residuals:[33] R = 0.056, R_w = 0.060, and GOF = 1.58.

Complex 6. X-ray quality crystals were grown from a saturated diethyl ether solution that was cooled to −30 °C. The final

cycle of full-matrix least squares refinement [minimizing the quantity $\Sigma w(|F_o| - |F_c|)^2$, where w is the weight of a given observation] was based on 2410 observed reflections [$I > 3.00\ \sigma(I)$] and 397 variable parameters and converged yielding final residuals:[33] $R = 0.052$, $R_w = 0.058$, and GOF = 1.59.

Complex 7. X-Ray quality crystals were grown from a saturated pentane solution that was cooled to −30 °C. The non-hydrogen atoms of the ordered portion of the model (the amidinate core of the ligand and the magnesium atom) were refined anisotropically, while the remaining carbon atoms (the disordered terphenyl unit) were refined isotropically (see text for more details). Hydrogen atoms were included for most carbon atoms but were not refined. The hydrogen atoms on carbon atoms that were present in both forms of the disorder (once as a methyl group, and once as an aromatic carbon) were omitted in the final model. The final cycle of full-matrix least squares refinement [minimizing the quantity $\Sigma w(|F_o| - |F_c|)^2$, where w is the weight of a given observation] was based on 1289 observed reflections [$I > 3.00\ \sigma(I)$] and 255 variable parameters and converged yielding final residuals:[33] $R = 0.133$, $R_w = 0.162$, and GOF = 4.74.

Complex 8. X-Ray quality crystals were grown from a saturated diethyl ether solution that was cooled to −30 °C. Most non-hydrogen atoms were refined anisotropically. Only the two carbon atoms that were modeled with 25% occupancy were refined isotropically. The final cycle of full-matrix least squares refinement [minimizing the quantity $\Sigma w(|F_o| - |F_c|)^2$, where w is the weight of a given observation] was based on 3017 observed reflections [$I > 3.00\ \sigma(I)$] and 450 variable parameters and converged yielding final residuals:[33] $R = 0.033$, $R_w = 0.044$, and GOF = 1.22.

CCDC reference numbers 181079–181083.

See http://www.rsc.org/suppdata/dt/b2/b202235b/ for crystallographic data in CIF or other electronic format.

Results and discussion

Sterically-hindered amidines

Recent studies have shown that terphenyl groups are capable of supporting unusual coordination environments,[23,34–46] the closest analogy to the work presented here being the formation of bulky carboxylate complexes.[47–49] Here, we report a set of three sterically-hindered amidine ligands, in which the steric bulk of the ligand system is derived from the attachment of terphenyl substituents on the central carbon atom of the amidinate backbone. Terphenyl moieties can be synthesized in a straightforward manner and on large scales (~100 g).[50] The synthesis proceeds through a benzyne intermediate to couple two equivalents of an aryl Grignard reagent to a trihalobenzene molecule, producing a *m*-terphenyl iodide product. In this manner, three terphenyl groups of varying steric bulk have been produced for use as precursors to sterically-bulky amidine ligands, including 2,6-bis(mesityl)iodobenzene [$R^1 = R^2 = Me$], 2,6-bis(2,4,6-triisopropylphenyl)iodobenzene [$R^1 = R^2 = {}^iPr$], and 2,6-bis(4-*tert*-butylphenyl)iodobenzene [$R^1 = H$, $R^2 = {}^tBu$] (Scheme 1).

From the terphenyl iodide precursors, the amidine ligands can be readily synthesized. Initially, lithiation is effected by suspending the terphenyl iodide in pentane and adding a solution of *n*-BuLi, giving the terphenyl lithium species in nearly quantitative yields as cream precipitates (Scheme 1). Without further purification, these precipitates, when dissolved in diethyl ether, insert one equivalent of diisopropylcarbodiimide to form the corresponding lithium amidinates. Quenching of the reaction mixture with water provides for routine workup and excellent yields (> 80%) of the pure amidine ligands: $\mathbf{L_{Me}H}$ [$R^1 = R^2 =$ Me] (**1**), $\mathbf{L_{^iPr}H}$ [$R_1 = R_2 = {}^iPr$] (**2**), and $\mathbf{L_{^tBu}H}$ [$R^1 = H$, $R^2 = {}^tBu$] (**3**).

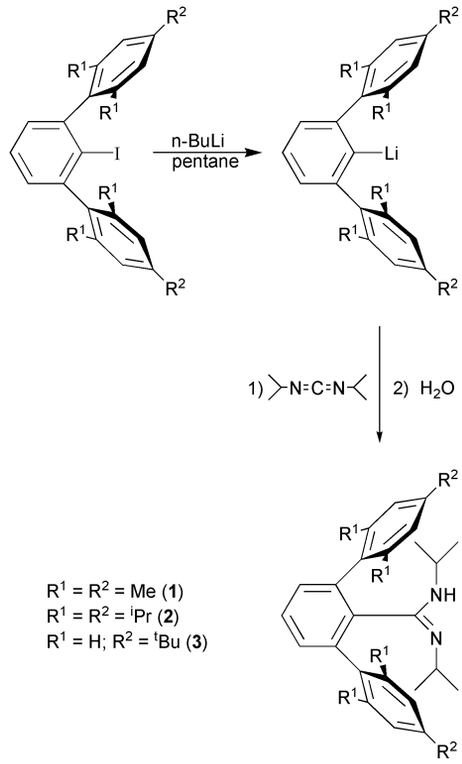

Scheme 1

NMR spectroscopic characterization showed some unexpected differences within this family of three ligands. The ^1H NMR spectrum of **1** is quite complex at room temperature, showing twice the expected number of amidine resonances.[21] TOCSY data allowed for deconvolution of the ^1H NMR resonances into two independent sets of peaks. The four isopropyl resonances are differentiated into two pairs: one pair from the imine nitrogen and one pair from the amine nitrogen. A NOESY spectrum showed chemical exchange between the two isopropyl groups within each pair, but not between the two pairs.[51] This exchange is attributed to interconversion between the *Z-syn* and *E-syn* isomers on the NMR timescale (Fig. 3),

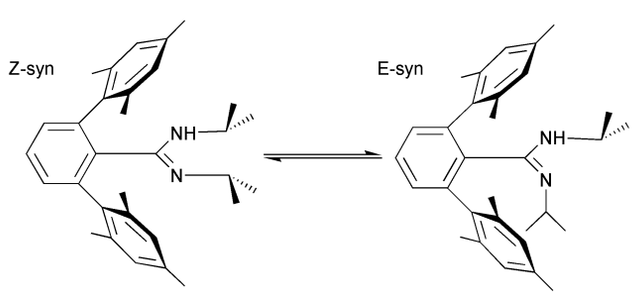

Fig. 3 Equilibrium isomerisation of **1** in solution at ambient temperature.

similar to the effects seen in *N*,*N*′-bis(2,6-diisopropylphenyl)-benzamidines.[20] The two equilibrated species can also be observed in the ^{13}C NMR spectrum for $\mathbf{L_{Me}H}$.

In contrast, in the cases of the ^{i}Pr and ^{t}Bu substituted ligands (**2** and **3**), the ^1H and ^{13}C spectra showed only one isomer and were consistent with free rotation about the bond linking the terphenyl group to the amidine backbone.[52] This rotation rendered the two halves of the terphenyl group chemically equivalent. Both also show a localized double-bond in the amidine backbone, as indicated by inequivalent isopropyl groups. In order to allow for the rapid rotation of the terphenyl group in **2**, we propose an exclusively *Z-syn* geometry for this species, even though this orientation is energetically less favored in smaller amidinates.[53] In this way, a trend can be derived, with the least

sterically demanding **3** exhibiting rapid equilibrium between *E-syn* and *Z-syn* isomers, as observed in non-bulky amidinate ligands. Increasing the steric bulk of the amidine slows down this equilibrium in **1**, and the *Z-syn* configuration is found to dominate in the very sterically encumbering amidine **2**.

X-Ray quality crystals of **1** were grown by slow cooling of a saturated pentane solution and the crystal structure of this bulky amidine ligand was obtained. Though **1** crystallized in a monomeric fashion, with no observed intermolecular hydrogen bonding interactions, it exhibits a substantial 'umbrella disorder'. The terphenyl group, with its large steric bulk, acts to shield the amidine functionality from crystal packing effects. Thus, similar to the solution phase, in the solid state the amidine exists in the two conformations (*E-syn* and *Z-syn*). Unfortunately, all attempts to model the occupancies of these two states were unsuccessful, as the *Z-syn* state dominates the population within the crystal. Therefore, the final crystallographic model includes full occupancy of the *Z-syn* state only, as shown in Fig. 4. The bond distances and angles for the *Z-syn*

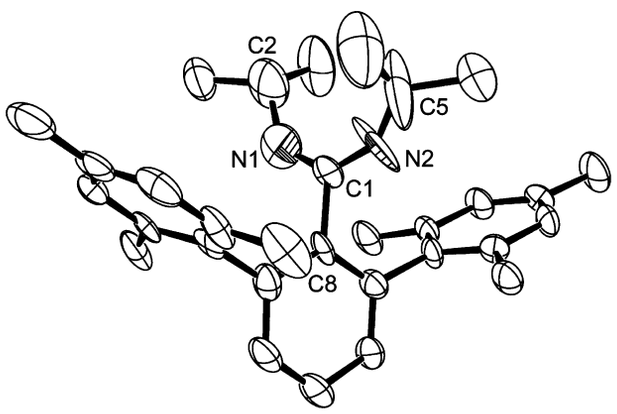

Fig. 4 ORTEP view of $L_{Me}H$ (**1**) drawn with 50% thermal ellipsoids. Selected bond lengths (Å): N1–C1 1.309(9), N2–C1 1.436(9), C1–C8 1.480(8); bond angles (°): N1–C1–N2 134.8(7), N1–C1–C8 116.6(7), N2–C1–C8 108.6(6).

isomer all fall within the typical ranges for amidine ligands.[1] As can be observed in the metrical parameters, the N(1)–C(1) bond has double bond character [1.309(9) Å], while N(2)–C(1) appears to be a single bond [1.436(9) Å]. Although the three bonds about C(1) deviate far from the idealized value of 120°, the sum of angles is 360.0(7)°, as expected for an sp^2 hybridized carbon atom.

Lithium complexes

Each of the amidines reacts readily with *n*-BuLi in ether to rapidly generate the corresponding lithium amidinate complex. Although they are difficult to crystallize as etherate complexes, upon exposure to tetramethylethylenediamine (TMEDA) the complexes crystallize well from saturated ether (**4**, **6**) or pentane (**5**) solutions. In this fashion, lithium salts of each of the three ligands of the general formula, (L^R)Li(TMEDA) [$R^1 = R^2$ = Me (**4**); $R^1 = R^2 = {}^i$Pr (**5**); R^1 = H, $R^2 = {}^t$Bu (**6**)] (Scheme 2) were obtained.

NMR spectra of the three complexes differed remarkably, despite the similarities between the ligands. Considering first the ^{t}Bu-substituted ligand (**6**), the NMR spectrum showed a highly symmetric species in which both halves of the amidinate ligand were spectroscopically equivalent, as expected. This is representative of a lithium amidinate complex where both nitrogen atoms coordinate to the lithium atom equally, and the N–C–N backbone of the amidinate contains a fully delocalized double bond. Additionally, rapid rotation about the bonds connecting the aryl rings of the terphenyl substituents allows for the equilibration of the remaining symmetric protons in the

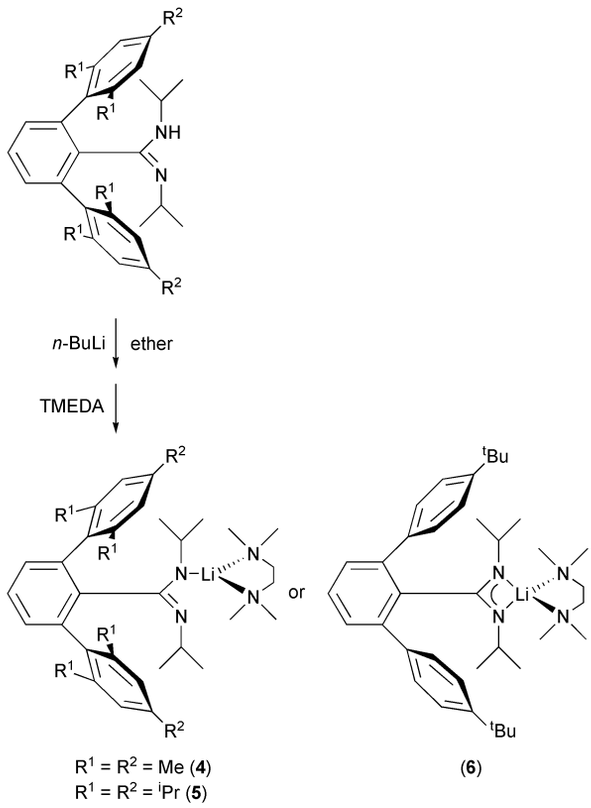

Scheme 2

compound. The coordinated molecule of TMEDA also has twofold symmetry. These characteristics are in agreement with the expected tetrahedrally-coordinated lithium (C_{2v} symmetry), in which the coordination sphere is composed of a pair of nitrogen atoms from each of the amidinate and TMEDA ligands, as has been observed in previous amidinate chemistry.[54,55]

In order to fully confirm the geometry of **6**, X-ray quality crystals were grown by slow cooling of a saturated diethyl ether solution. The crystals grew as large blocks and provided excellent diffraction data. The resulting structure confirmed the expected tetrahedral coordination geometry at the lithium atom (Fig. 5). The amidinate ligand and the TMEDA both bind to the

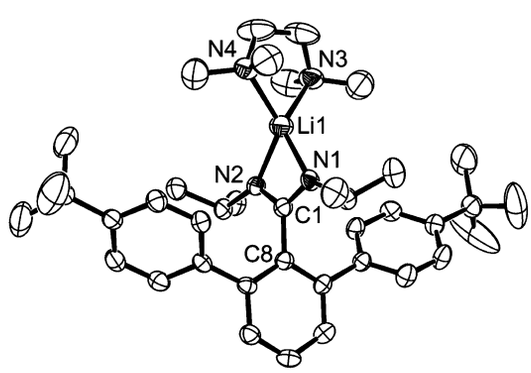

Fig. 5 ORTEP view of L_{Bu}Li(TMEDA) (**6**) drawn with 50% thermal ellipsoids. Selected bond lengths (Å): Li–N1 1.995(9), Li1–N2 1.998(9), Li1–N3 2.086(9), Li1–N4 2.109(9), N1–C1 1.329(5), N2–C1 1.327(5), C1–C8 1.530(6); bond angles (°): N1–Li1–N2 68.8(3), N1–Li1–N3 130.1(5), N1–Li1–N4 124.7(4), N2–Li1–N3 123.6(5), N2–Li1–N4 129.5(5), N3–Li1–N4 86.5(4), N1–C1–N2 116.3(4).

lithium atom in a symmetric bidentate fashion. No disorder was present, allowing for accurate determination of metrical parameters for this compound. The amidinate–lithium (1.99 Å) and TMEDA–lithium (2.09, 2.11 Å) bond lengths of **6** are well within the range seen in other amidinate lithium complexes.[54–58]

The amidinate N–Li–N (68.8°) and N–C–N (116.3°) angles are quite similar to those found in related species.[54,55] These values, therefore, appear to be only minimally affected by the incorporation of the bulky terphenyl substituent in the ligand backbone of **6**.

As previously reported, the ^{1}H NMR spectrum of **4** shows the formation of a much less symmetric species.[21] In this case, two different ^{i}Pr resonances, three inequivalent mesityl methyls, and two independent mesityl aromatic signals are observed, indicating an unsymmetrical product with C_s symmetry. The ^{13}C NMR spectrum shows a similar reduced symmetry, consistent with the overall C_s symmetry of this molecule. The coordinated TMEDA ligand shows twofold symmetry in both the proton and carbon NMR spectra. These data were indicative of monodentate binding of the bulky amidinate to the lithium ion, a phenomenon that had not previously been observed for lithium amidinates. As a definitive means of determining the bonding mode in **4**, X-ray quality crystals were grown from a diethyl ether solution, and the solid-state structure of (L_{Me})Li(TMEDA) shows that the amidinate is coordinated through only one nitrogen atom, as detailed previously.[21] There are two potential causes of the unusual lithium coordination in **4**, both of which we ascribe to steric effects: (i) crowding caused by interaction of the TMEDA with the *ortho* substituents of the terphenyl substituent on the amidinate ligand and (ii) interaction of the terphenyl substituents with the N-bound ^{i}Pr groups. Of the two, we suspect the latter dominates, resulting in one of the two N-^{i}Pr groups residing in a geometry unfavorable for coordination to Li.

The NMR spectra of the remaining lithium amidinate (**5**) were very similar to those observed for the unsymmetrical product, **4**. Again, C_s symmetry was observed in both the proton and carbon spectra for all of the ligand resonances. Also, analogously to **4**, the TMEDA signals were indicative of twofold symmetry within this ligand. Thus, a coordination environment involving monodentate coordination of the amidinate ligand was again invoked in this species.

Confirmation of this coordination geometry was achieved by X-ray crystallography. Suitable crystals of **5** were achieved by slow cooling of a saturated pentane solution. The structure of this compound is analogous to that observed for **4** with a three-coordinate lithium atom, coordinated in a bidentate fashion by the TMEDA moiety and by one nitrogen of the amidinate ligand (Fig. 6). Again, the lithium atom resides in a

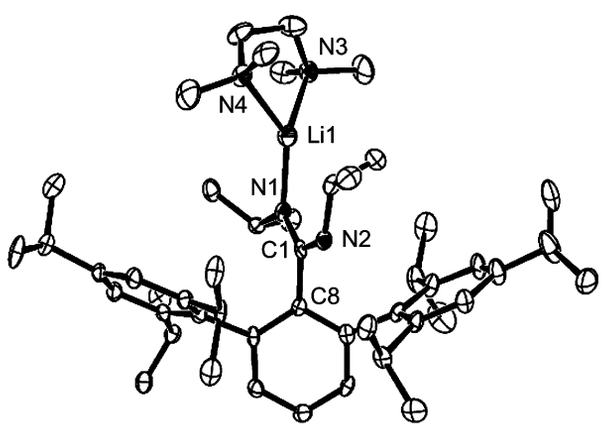

Fig. 6 ORTEP view of L_{Pr}Li(TMEDA) (**5**) drawn with 50% thermal ellipsoids. Selected bond lengths (Å): Li1–N1 1.978(8), Li1–N3 2.181(8), Li–N4 2.257(7), N1–C1 1.361(5), N2–C1 1.309(5), C1–C8 1.516(5); bond angles (°): N1–Li1–N3 135.5(3), N1–Li1–N4 134.7(4), N3–Li1–N4 84.2(3), N1–C1–N2 123.6(4).

distorted trigonal planar environment [sum of angles around lithium = 354.4(4)°], though much further from the ideal 360° than was observed in the previous example (**4**). The double-bond localization within the backbone of **5** is much more pronounced than was observed for **4** [C(1)–N(1) 1.361(5) Å, C(1)–N(2) 1.309(5) Å]. The bond between the amidinate and the lithium ion [N(1)–Li(1) 1.978(8)Å] is slightly longer than that observed for **4**. This lengthening may be attributed to increased steric interactions between the bulky amidinate ligand and the TMEDA ligand. Additionally, the N(TMEDA)–Li bonds (2.181 and 2.257 Å) are somewhat longer than those in **4**, although they remain within the range of bond lengths observed in other Li(TMEDA)$^+$ containing species. It appears that the replacement of the *ortho* methyl substituents in **4** with isopropyl groups in **5** seems to have a strong steric effect on the bonding of this ligand, creating an even more sterically strained environment than was found in **4**.

Magnesium complexes

We chose to investigate synthetic routes to magnesium salts of the sterically-hindered amidinate ligands as potential precursors to transition metal complexes. These salts are potentially useful in lanthanide chemistry, where unwanted lithium salts released in metathesis reactions are often incorporated in the final product. Amidine **1** reacted cleanly with 0.5 equivalents of dibutylmagnesium in toluene to form the bis(amidinate) complex, (L_{Me})$_2$Mg (**7**) in moderate yield (Scheme 3).

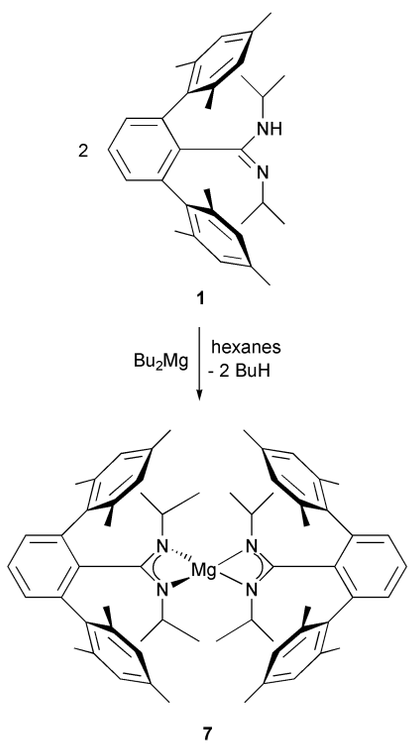

Scheme 3

This highly soluble compound was recrystallized from hexanes as clear, colorless crystalline blocks. The ^{1}H NMR spectrum of **7** showed resonances indicative of a highly symmetric complex in which the two amidinates were equivalent and within each a twofold rotational symmetry equilibrated the two halves of the ligand. Thus, **7** was assigned a tetrahedral geometry in which four nitrogen atoms from the two ligands coordinate to the magnesium. The ^{13}C NMR spectrum supported this arrangement, and the presence of a peak at 903 *m*/*z* in the EI mass spectrum of this compound confirmed the formulation of this bis-amidinate species.

X-Ray quality crystals of **7** were grown, and the crystal structure of this species was solved. Unfortunately, the packing of these crystals resulted in a twofold disorder of the terphenyl group in the ligand (Fig. 7). There were two positions for the terphenyl group, and these were modeled with 50% occupancy

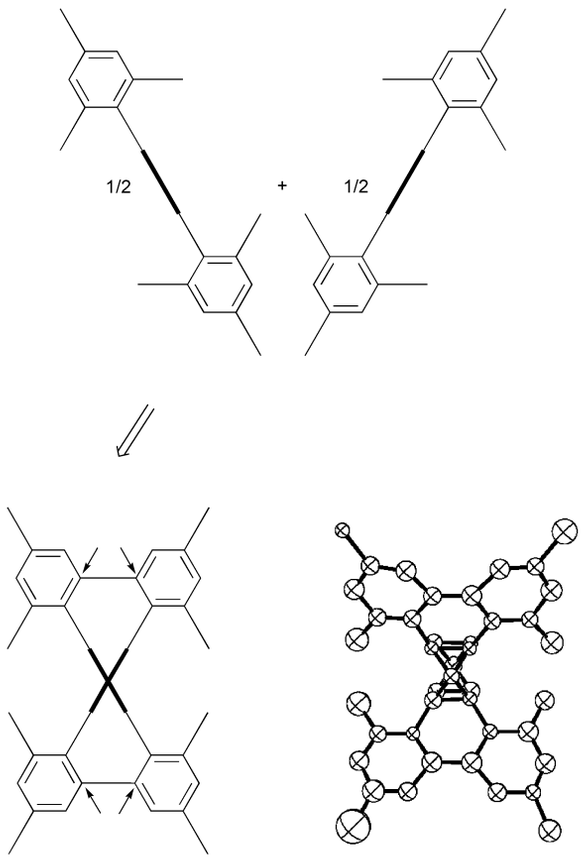

Fig. 7 Line diagrams and final ORTEP model showing the two-fold disorder present in the terphenyl backbone of the ligand in compound **7**.

each. As shown in the figure, four of the modeled carbon atoms are methyl groups in one orientation and aromatic carbons in the second, while two of the central phenyl carbon atoms are shared by both rotamers. The net result of this disorder is a solution in which the positional locations of the atoms of the terphenyl moiety are only poorly determined and bond lengths and angles related to these atoms are of only dubious value. Fortunately, the core of this molecule is well ordered, allowing for refinement of the $(^{i}PrNCN^{i}Pr)_2Mg$ portion of the molecule (Fig. 8). Equal Mg–N bond lengths [2.04(1) Å] were observed

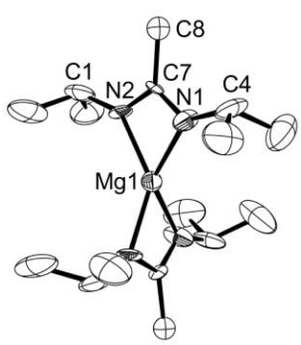

Fig. 8 ORTEP view of the ordered core of $(L_{Me})_2Mg$ (**7**) drawn with 50% thermal ellipsoids. Selected bond lengths (Å): Mg1–N1 2.04(1), Mg1–N2 2.04(1), N1–C7 1.31(2), N2–C7 1.31(2), C7–C8 1.52(2); bond angles (°): N1–Mg1–N2 64.2(7), N1–Mg1–N1* 133(1), N1–Mg1–N2* 134.9(7), N2–Mg1–N2* 139(1), N1–C7–N2 111(1).

and bond angles of 111(1)° (N–C–N) and 64.2(7)° (N–Mg–N) were present. The Mg–N bond lengths are shortened compared to previously characterized magnesium amidinates, which is likely an effect of the reduced coordination number at Mg, as all previous crystallographically characterized magnesium amidinates contain coordination numbers of five or more.[59–64] The N–C–N bond angle is slightly more acute than those observed previously in magnesium amidinates, probably due to the increased steric bulk of this ligand. The steric interactions between the isopropyls and the terphenyl group prevent the ligand from opening to the larger N–C–N angles found in less bulky systems.

By using an alternate synthetic route, a monoamidinate magnesium complex deriving from **3** was obtained. In this case, the Grignard reagent formed by reacting the terphenyliodide with Mg was reacted directly with one equivalent of diisopropylcarbo-diimide, yielding the amidinate (Scheme 4). After

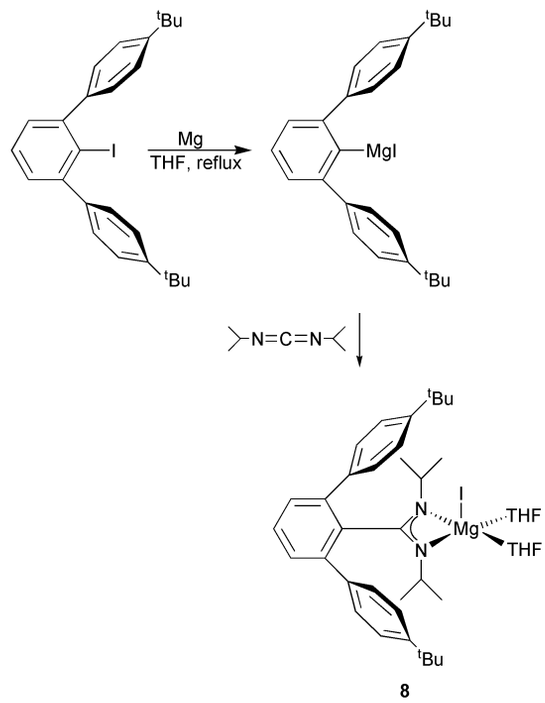

8

Scheme 4

removal of the THF solvent, the remaining white solid was extracted with ether. Concentration and cooling of this solution gave clear colorless crystals of $(L_{Bu})MgI(THF)_2$ (**8**) in moderate yield. Again, the ^1H NMR spectrum showed a symmetric amidinate ligand with two equivalent halves on the NMR timescale. Also, two broad resonances integrating to eight protons each were representative of the pair of coordinated THF molecules. The ^{13}C NMR showed the appropriate set of resonances, consistent with this formulation for **8**.

Colorless crystals of **8** obtained by crystallization of this species from diethyl ether were suitable for X-ray crystal structure determination. The solid-state structure confirmed the initial formulation, showing magnesium coordinated by both nitrogen atoms of an amidinate ligand, one iodide, and two oxygen atoms from ethereal solvent (Fig. 9). Because of the crystallization conditions employed, the final crystallographic model includes 1.25 equivalents of THF and 0.75 equivalents of ether coordinated to the Mg. Other than this simple solvent exchange disorder, the crystal structure was ordered and refined well. The structure shows the magnesium coordinated in an approximately square pyramidal coordination environment with the iodine located in the apical position. This is consistent with the solution NMR data, as this coordination geometry yields an approximate mirror plane through the center of the amidinate and rotation of the terphenyl group completes the equilibration of the two halves of the ligand. In comparison to $(L_{Me})_2Mg$ (**7**), **8** contains slightly longer Mg–N bond lengths of 2.085(6) and 2.140(6) Å and very similar bond angles of 114.5(6)° (NCN) and 64.3(2)° (NMgN), all of which are well

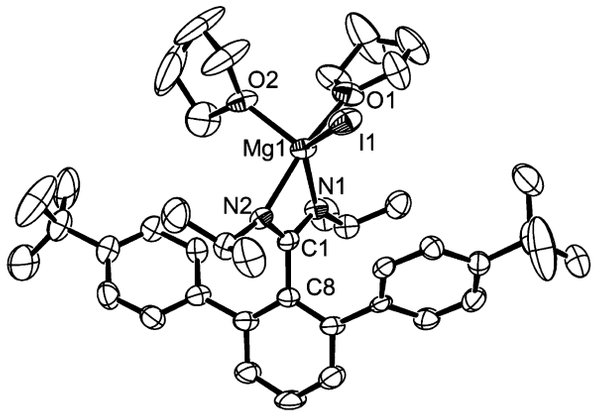

Fig. 9 ORTEP view of $L_{Bu}MgI(THF)_2$ (**8**) drawn with 50% thermal ellipsoids. Selected bond lengths (Å): Mg1–N1 2.085(6), Mg1–N2 2.140(6), Mg1–I1 2.783(2), Mg–O1 2.120(5), Mg1–O2 2.083(5), N1–C1 1.339(8), N2–C1 1.332(8), C1–C8 1.513(9); bond angles (°): N1–Mg1–N2 64.3(2), N1–Mg1–I1 132.4(2), N1–Mg1–O1 98.3(2), N1–Mg1–O2 117.7(2), N2–Mg1–I1 102.1(2), N2–Mg1–O1 162.1(2), N2–Mg1–O2 98.8(2), I1–Mg1–O1 92.5(2), I1–Mg1–O2 109.3(2), O1–Mg1–O2 85.5(2), N1–C1–N2 114.5(6).

within the range of previously observed values for magnesium amidinate complexes.[59–64]

Conclusions

Sterically hindered amidinate ligands can be readily synthesized in high yields, on large scales, and in pure form, from known terphenyl iodide starting materials. From these, lithium amidinate complexes were readily synthesized and, by crystallization in the presence of TMEDA, pure crystalline lithium amidinate species were isolated. Additionally, two independent routes to the formation of magnesium amidinates have been developed to produce either mono- or bis-amidinate magnesium complexes. In future publications, the use of these precursors for the formation of metal complexes and their organometallic chemistry will be reported.

The use of terphenyl substituents at the carbon atom of the amidinate backbone seems to produce a strong steric effect on these ligand systems. This was observed in each of the three forms of the ligand demonstrated here. In the free-base amidines, the equilibria between *E-syn* and *Z-syn* isomers were strongly affected by steric interactions between the terphenyl moiety and the isopropyl groups attached to the amidine core. In the lithium amidinates, the steric bulk of these ligands led to the formation of the first monodentate lithium amidinates. Finally, in the magnesium amidinates, these steric effects led to shortened bond lengths and reduced bond angles within the amidinate backbone due to the coordination environments that these ligands provide.

Acknowledgements

The authors gratefully acknowledge the NSF for funding, the Department of Defense Science and Engineering Graduate (NDSEG) Fellowship Program for fellowship support (J. A. R. S.), as well as Doctors Fred Hollander and Allen Oliver for insightful discussions.

References and notes

1 J. Barker and M. Kilner, *Coord. Chem. Rev.*, 1994, **133**, 219.
2 J. R. Hagadorn and J. Arnold, *Organometallics*, 1998, **17**, 1355.
3 G. D. Whitener, J. R. Hagadorn and J. Arnold, *J. Chem. Soc., Dalton Trans.*, 1999, 1249.
4 F. A. Cotton, C. A. Murillo and I. Pascual, *Inorg. Chem.*, 1999, **38**, 2182.
5 R. D. Simpson and W. J. Marshall, *Organometallics*, 1997, **16**, 3719.
6 K. Shibayama, S. W. Seidel and B. M. Novak, *Macromolecules*, 1997, **30**, 3159.
7 Y. L. Zhou and D. S. Richeson, *Inorg. Chem.*, 1997, **36**, 501.
8 S. M. Mullins, J. R. Hagadorn, R. G. Bergman and J. Arnold, *J. Organomet. Chem.*, 2000, **607**, 227.
9 S. M. Mullins, R. G. Bergman and J. Arnold, *Organometallics*, 1999, **18**, 4465.
10 D. Y. Dawson and J. Arnold, *Organometallics*, 1997, **16**, 1111.
11 J. R. Hagadorn and J. Arnold, *J. Chem. Soc., Dalton Trans.*, 1997, 3087.
12 J. R. Hagadorn and J. Arnold, *Organometallics*, 1994, **13**, 4670.
13 J. R. Hagadorn and J. Arnold, *Angew. Chem., Int. Ed.*, 1998, **37**, 1729.
14 J. R. Hagadorn and J. Arnold, *J. Am. Chem. Soc.*, 1996, **118**, 893.
15 J. R. Hagadorn and J. Arnold, *Organometallics*, 1996, **15**, 984.
16 K. Kincaid, C. P. Gerlach, G. R. Giesbrecht, J. R. Hagadorn, G. D. Whitener, A. Shafir and J. Arnold, *Organometallics*, 1999, **18**, 5360.
17 J. R. Hagadorn and J. Arnold, *Inorg. Chem.*, 1997, **36**, 132.
18 M. P. Coles, D. C. Swenson, R. F. Jordan and V. G. Young, *Organometallics*, 1997, **16**, 5183.
19 M. P. Coles, D. C. Swenson, R. F. Jordan and V. G. Young, *Organometallics*, 1998, **17**, 4042.
20 R. T. Boeré, V. Klassen and G. Wolmershauser, *J. Chem. Soc., Dalton Trans.*, 1998, 4147.
21 J. A. R. Schmidt and J. Arnold, *Chem. Commun.*, 1999, 2149.
22 While we were investigating this system, the synthesis of a related bulky amidinate aluminium dimethyl species was reported: D. Abeysekera, K. N. Robertson, T. S. Cameron and J. A. C. Clyburne, *Organometallics*, 2001, **20**, 5532.
23 B. Schiemenz and P. P. Power, *Organometallics*, 1996, **15**, 958.
24 L. J. Farrugia, *J. Appl. Crystallogr.*, 1997, **30**, 565.
25 SMART: Area-Detector Software Package, Siemens Industrial Automation, Inc., Madison, WI, 1995.
26 SAINT: SAX Area-Detector Integration Program, V4.024, Siemens Industrial Automation, Inc., Madison, WI, 1995.
27 XPREP: Part of the SHELXTL Crystal Structure Determination Package, V5.03, Siemens Industrial Automation, Inc., Madison, WI, 1995.
28 A. Altomare, G. Cascarano, C. Giacovazzo and A. Guagliardi, *J. Appl. Crystallogr.*, 1993, **26**, 343.
29 The DIRDIF Program System, Technical Report of the Crystallography Laboratory, University of Nijmegen, 1992.
30 teXsan: Crystal Structure Analysis Package, Molecular Structure Corporation, Houston, TX, 1992.
31 D. T. Cromer and J. T. Waber, *International Tables for X-Ray Crystallography*, Kynoch Press, Birmingham, 1974.
32 J. A. Ibers and W. C. Hamilton, *Acta Crystallogr.*, 1964, **17**, 781.
33 $R = \Sigma||F_o| - |F_c||/\Sigma|F_o|$, $R_w = [(\Sigma w(|F_o| - |F_c|)^2/\Sigma w F_o^2)]^{1/2}$, GOF = $[\Sigma w(|F_o| - |F_c|)^2/(N_o - N_v)]^{1/2}$ where N_o = number of observations and N_v = number of variables and the weight $w = 4\ F_o^2/\sigma^2(F_o)^2 = [\sigma^2(F_o) + (pF_o/2)^2]^{-1}$ and p is the factor used to lower the weight of intense reflections.
34 B. Twamley, C. D. Sofield, M. M. Olmstead and P. P. Power, *J. Am. Chem. Soc.*, 1999, **121**, 3357.
35 J. R. Su, X. W. Li, R. C. Crittendon and G. H. Robinson, *J. Am. Chem. Soc.*, 1997, **119**, 5471.
36 X. M. He, R. A. Bartlett, M. M. Olmstead, K. Ruhlandt-Senge, B. E. Sturgeon and P. P. Power, *Angew. Chem., Int. Ed. Engl.*, 1993, **32**, 717.
37 B. E. Eichler and P. P. Power, *Inorg. Chem.*, 2000, **39**, 5444.
38 L. H. Pu, B. Twamley and P. P. Power, *Organometallics*, 2000, **19**, 2874.
39 B. E. Eichler, N. J. Hardman and P. P. Power, *Angew. Chem., Int. Ed.*, 2000, **39**, 383.
40 N. J. Hardman, B. Twamley and P. P. Power, *Angew. Chem., Int. Ed.*, 2000, **39**, 2771.
41 B. E. Eichler and P. P. Power, *J. Am. Chem. Soc.*, 2000, **122**, 8785.
42 L. H. Pu, P. P. Power, I. Boltes and R. Herbst-Irmer, *Organometallics*, 2000, **19**, 352.
43 C. S. Hwang and P. P. Power, *J. Am. Chem. Soc.*, 1998, **120**, 6409.
44 B. Twamley, C. S. Hwang, N. J. Hardman and P. P. Power, *J. Organomet. Chem.*, 2000, **609**, 152.
45 S. T. Haubrich and P. P. Power, *J. Am. Chem. Soc.*, 1998, **120**, 2202.
46 B. Twamley and P. P. Power, *Angew. Chem., Int. Ed.*, 2000, **39**, 3500.
47 J. R. Hagadorn, L. Que and W. B. Tolman, *J. Am. Chem. Soc.*, 1998, **120**, 13531.
48 D. W. Lee and S. J. Lippard, *J. Am. Chem. Soc.*, 1998, **120**, 12153.
49 J. R. Hagadorn, L. Que and W. B. Tolman, *Inorg. Chem.*, 2000, **39**, 6086.
50 C. J. F. Du, H. Hart and K. K. D. Ng, *J. Org. Chem.*, 1986, **51**, 3162.

51 J. K. M. Sanders and B. K. Hunter, *Modern NMR Spectroscopy: A Guide for Chemists*, Oxford University Press, New York, 1993.
52 A small amount (< 10%) of a second species can be observed in equilibrium in **2** but is not present in large enough amounts to adequately characterize spectroscopically. These resonances are attributed to the sterically less-favorable *E-syn* isomer.
53 S. Patai and Z. Rappoport, *The Chemistry of Amidines and Imidates*, Wiley, New York, 1991.
54 J. Barker, D. Barr, N. D. R. Barnett, W. Clegg, I. Cragg-Hine, M. G. Davidson, R. P. Davies, S. M. Hodgson, J. A. K. Howard, M. Kilner, C. W. Lehmann, I. Lopez-Solera, R. E. Mulvey, P. R. Raithby and R. Snaith, *J. Chem. Soc., Dalton Trans.*, 1997, 951.
55 C. Averbuj, E. Tish and M. S. Eisen, *J. Am. Chem. Soc.*, 1998, **120**, 8640.
56 L. M. Engelhardt, G. E. Jacobsen, P. C. Junk, C. L. Raston, B. W. Skelton and A. H. White, *J. Chem. Soc., Dalton Trans.*, 1988, 1011.
57 I. Cragg-Hine, M. G. Davidson, F. S. Mair, P. R. Raithby and R. Snaith, *J. Chem. Soc., Dalton Trans.*, 1993, 2423.
58 W. M. Boesveld, P. B. Hitchcock and M. F. Lappert, *J. Chem. Soc., Dalton Trans.*, 1999, 4041.
59 M. Westerhausen and H. D. Hausen, *Z. Anorg. Allg. Chem.*, 1992, **615**, 27.
60 M. D. Li, C. C. Chang, Y. Wang and G. H. Lee, *Organometallics*, 1996, **15**, 2571.
61 F. A. Cotton, S. C. Haefner, J. H. Matonic, X. P. Wang and C. A. Murillo, *Polyhedron*, 1997, **16**, 541.
62 B. Srinivas, C. C. Chang, C. H. Chen, M. Y. Chiang, I. T. Chen, Y. Wang and G. H. Lee, *J. Chem. Soc., Dalton Trans.*, 1997, 957.
63 A. R. Kennedy, R. E. Mulvey and R. B. Rowlings, *J. Am. Chem. Soc.*, 1998, **120**, 7816.
64 D. Walther, P. Gebhardt, R. Fischer, U. Kreher and H. Gorls, *Inorg. Chim. Acta*, 1998, **281**, 181.